

PAPER • OPEN ACCESS

## Structural investigation of epitaxial $\text{LaFeO}_3$ thin films on (111) oriented $\text{SrTiO}_3$ by transmission electron microscopy

To cite this article: E Christiansen *et al* 2015 *J. Phys.: Conf. Ser.* **644** 012002

View the [article online](#) for updates and enhancements.

### Related content

- [Enhancement of photocatalytic activities of perovskite  \$\text{LaFeO}\_3\$  composite by incorporating nanographene platelets](#)  
N Afifah and R Saleh
- [Preparation and Electrical Properties of  \$\text{LaFeO}\_3\$  Compacts Using Chemically Synthesized Powders](#)  
Sheng-Heng Chung, Kuo-Chuang Chiu and Jau-Ho Jean
- [Experimental and theoretical investigation of electronic structure of  \$\text{SrFeO}\_{3-x}\$  epitaxial thin films prepared via topotactic reaction](#)  
Tsukasa Katayama, Akira Chikamatsu, Hideyuki Kamisaka et al.

# Structural investigation of epitaxial LaFeO<sub>3</sub> thin films on (111) oriented SrTiO<sub>3</sub> by transmission electron microscopy

E Christiansen<sup>1</sup>, M Nord<sup>1</sup>, I Hallsteinsen<sup>2</sup>, P E Vullum<sup>1,3</sup>, T Tybell<sup>2</sup>, R Holmestad<sup>1</sup>.

<sup>1</sup> Department of Physics, Norwegian University of Science and Technology (NTNU), 7491 Trondheim, Norway.

<sup>2</sup> Department of Electronics and Telecommunications, Norwegian University of Science and Technology (NTNU), 7491 Trondheim, Norway.

<sup>3</sup> SINTEF, Materials and Chemistry, 7465 Trondheim, Norway.

E-mail: randi.holmestad@ntnu.no

**Abstract.** We report on structural domains in LaFeO<sub>3</sub> epitaxial thin films on (111) oriented SrTiO<sub>3</sub> observed by transmission electron microscopy using low magnification dark field imaging and high resolution transmission electron microscopy techniques. The films were grown by pulsed laser deposition and had a thickness  $\approx 20$  nm. Three domain orientations are found, in accordance with the orthorhombic structure of LaFeO<sub>3</sub>. The domains themselves are of irregular shapes, and vary in size from tens to thousands of nm<sup>2</sup>. Regions of reduced Bragg scattering are observed as straight lines along  $\langle 100 \rangle$ , hinting at a complex domain structure.

## 1. Introduction

Antiferromagnetic (AFM) materials play an important role in magnetic device technology, such as the spin valves [1]. In such devices, AFM layers are used to pin adjacent ferromagnetic layers through exchange coupling [2]. In order to apply novel functional magnetic systems in practical applications, such as magnetic data memory, thin films with sharp interfaces between the AFM and ferromagnetic layers are necessary [3]. Perovskite oxide materials are in this regard interesting, exhibiting functional properties including both ferromagnetic and antiferromagnetic systems [4]. Based on their strong structure-property coupling, the functional properties of perovskite thin films can be tailored by synthesis [5].

LaFeO<sub>3</sub> (LFO) is a G-type antiferromagnetic perovskite [6]. It belongs to the orthorhombic space group  $Pbnm$  (no. 62) and has lattice parameters  $a = 5.556$  Å,  $b = 5.565$  Å, and  $c = 7.862$  Å (pseudo cubic parameters  $a_{pc} = 3.929$  Å,  $b_{pc} = 3.935$  Å, and  $c_{pc} = 3.931$  Å) at room temperature, which makes it belong to the  $a_{pc}^- a_{pc}^- c_{pc}^+$  Glazer tilt system [7, 8]. This means that the oxygen octahedra are tilted out-of-phase along  $a_{pc}$  and  $b_{pc}$ , and in-phase along  $c_{pc}$ . Its Néel temperature of  $T_N = 740$  K is highest among the orthoferrites, and is attributed to the large buckling angle of the Fe-O-Fe bonds related to the octahedra tilts [9, 10]. For depositing LFO thin films, a common substrate is SrTiO<sub>3</sub> (STO), a nonmagnetic and insulating cubic  $Pm\bar{3}m$  (no. 221) perovskite with  $a_{STO} = 3.905$  Å (parameters and indices without a subscript are LFO indices



unless otherwise specified, while subscript *STO* is used to denote STO axes throughout this paper).

For thin films of LFO on (100) and (110) STO, the Néel temperature is slightly reduced [11]. Due to its orthorhombic symmetry, LFO forms structural domains on STO. Moreover, photoelectron emission microscopy data indicate AFM domains of the same shape and size as the structural domains. In the present work, the structure of an epitaxial thin film of LFO on (111) oriented STO grown by pulsed laser deposition (PLD) is studied by transmission electron microscopy (TEM). This in order to study possible effects off the quasi-hexagonal surface symmetry of this facet on structural domain formation. Domains in the film is studied by electron diffraction and dark field (DF) imaging of plan-view samples, and the LFO/STO interface is studied by high resolution TEM (HRTEM) of cross section samples.

## 2. Materials and methods

The LaFeO<sub>3</sub> thin film was synthesised by PLD, using a KrF excimer laser (wavelength  $\lambda = 248$  nm) with a fluency of  $\sim 2$  J/cm<sup>2</sup> and repetition rate 1 Hz impinging on a stoichiometric LaFeO<sub>3</sub> target. A deposition temperature of 540 °C, oxygen pressure of 0.35 mbar and target-substrate distance of 45 mm was used to ensure quality growth [12]. The substrate was prepared by buffered hydrogen fluoride etch and annealing in oxygen ambient, resulting in a step and terrace structure with miscut of 0.1° and step edges along a  $\langle 11\bar{2} \rangle$  STO direction. Reflection high energy electron diffraction was used to monitor the growth in situ, ensuring layer-by-layer growth. Atomic force microscopy confirmed a high surface quality of the film, and the film was found to be fully epitaxial by x-ray diffraction.

TEM samples of both plan-view and cross section geometries were prepared. Plan-view samples were fabricated by grinding film wafer pieces from the substrate side into a wedge shape (wedge angle of 4°), using an *Allied MultiPrep Polishing System* (tripod). One plan-view sample was further thinned in a *FEI Helios NanoLab DualBeam FIB* in order to remove surface scratches from the tripod polishing, and provide unbent electron transparent regions. Pure tripod plan-view samples were also fabricated to control that the FIB process did not alter the structure of the film. The sample that was Ga<sup>+</sup> ion-beam thinned yielded the same results as samples prepared solely by tripod polishing, demonstrating that ion-beam thinning did not alter the crystallography of the material system. All presented images are from samples that were prepared by low energy (2 kV) ion-beam thinning, as pure mechanical polishing leaves polishing stripes and other surface defects. The same FIB instrument was used to fabricate cross section samples from the same film, using a lift-out procedure.

Dark field imaging was performed on a *JEOL JEM-2100* LaB<sub>6</sub> TEM. In order to better show and compare the relationships between the three different structural domains, several DF images taken with each of the unique orthorhombic reflections were merged into a single image. Domains with equal crystallographic orientations are given the same colour (see Fig. 1). For HRTEM imaging a *JEOL JEM-2100F* field emission gun TEM was used. Both TEMs were operated at 200 kV acceleration voltages.

## 3. Results and discussion

A domain mosaic, combining six DF images from a plan-view sample, is presented in Fig. 1. The six DF images are taken with each of the six orthorhombic super reflections, located midway between 000 and each of the six  $\langle 1\bar{1}0 \rangle_{STO}$  reflections. Since the TEM sample is a bilayer with the 20 nm thick LFO film on top of the substrate, the electron beam will pass through both the film and the substrate and the resulting diffraction pattern will thus contain information about both layers simultaneously. However, the reflections chosen for each of the dark field images are unique for the LFO film and not present in the diffraction pattern from pure STO. As such, the contrast from elastic Bragg scattering in the DF images will only come from the LFO film.

Furthermore, the chosen DF reflections are the orthorhombic 100 or 010 reflections. This also means that we have at least three different structural domains in the LFO film. Each structural domain contributes to two of the six super reflections. The domain mosaic in Fig. 1 is composed of six DF images, even if three theoretically would be enough, but using all six reflections helps to cancel out contrast changes due to sample bending that will give small variations of the sample orientation.

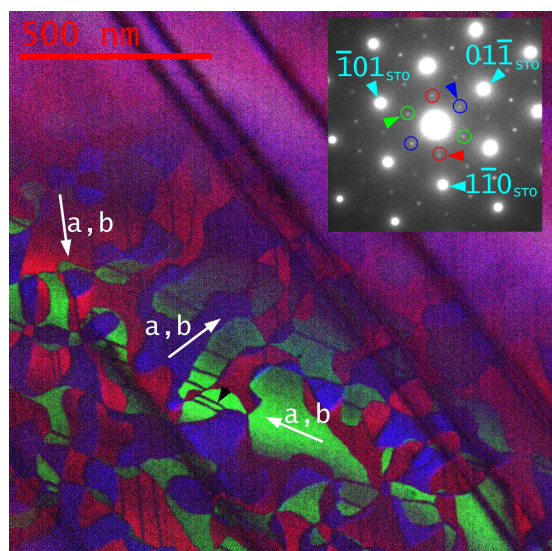


**Figure 1.** DF mosaic of six individual DF images. The reflections used are circled in the inset electron diffraction pattern, the colour of the circles indicate the colour assigned to each DF image. The arrowheads in the diffraction pattern mark LFO (100)/(010) reflections, and the white arrows in the real space image show the direction of [100]/[010]. Dark lines are seen inside some domains, one case being pointed out by a black arrowhead. Such lines tend to be parallel to [100]/[010].

In Fig. 1 we observe that the orthorhombic [100] or [010] directions can be parallel to  $[1\bar{1}0]_{STO}$ ,  $[\bar{1}01]_{STO}$  or  $[01\bar{1}]_{STO}$ , leading to the three different structural domains with red, green and blue colours in the figure, respectively. However, we are not able to discriminate between the orthorhombic [100] and [010] directions since the orthorhombic  $a$  and  $b$  lattice parameters are almost equal. This means that two regions with the same colour in Fig. 1 does not necessary have the same orientation of the unit cell, as the orthorhombic  $a$  and  $b$  lattice parameters can switch between any two regions with the same colour. We also observe lines inside one-coloured regions where we have insignificant Bragg scattering to any of the six super reflections. If these lines are related to for instance twin boundaries where the orthorhombic  $a$  and  $b$  lattice parameters switch directions across the dark line, is something that future characterization work must answer.

A HRTEM image from a cross section sample with  $[11\bar{2}]_{STO}$  zone axis orientation is presented in Fig. 2, revealing a coherent film/substrate interface and high crystalline quality film. The Fourier transforms (inset in the HRTEM image) from the left (region A) and the right (region B) sides of the film clearly show that more than one structural domain are present in the field of view. In region A we have a structural domain where the orthorhombic  $a$  or  $b$  lattice parameter is parallel to the  $[1\bar{1}0]$  direction of STO. In region B the orthorhombic unit cell is oriented differently with none of the orthorhombic lattice parameters being parallel to the  $[1\bar{1}0]_{STO}$  direction.

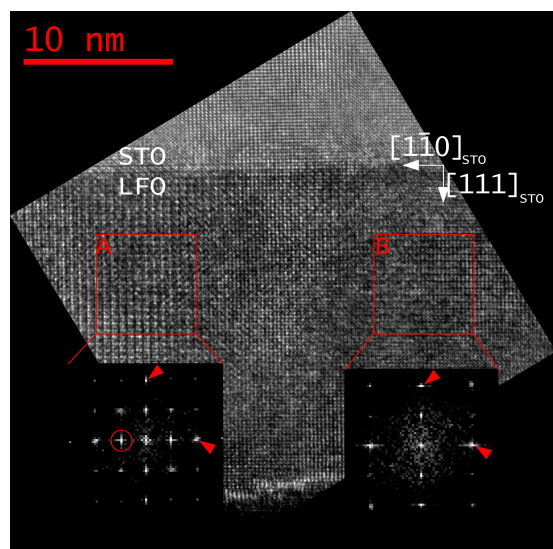


**Figure 2.** HRTEM image of LFO thin film cross section sample acquired in the  $[11\bar{2}]_{STO}$  zone axis. The film is epitaxial, but not structurally homogeneous, as the FFT spectra of region "A" and "B" are clearly different, indicating the presence of at least two different domains. The lowest spatial frequencies of STO have been marked by arrowheads for reference. The circled frequency component in the FFT of region A indicates that either  $a$  or  $b$  is aligned with the  $[\bar{1}10]_{STO}$  direction in this domain. As region B lacks this frequency component, the  $a$  or  $b$  axis may not be parallel to the  $[\bar{1}10]_{STO}$  direction here.

#### 4. Conclusions

Structural domains of irregular shape and size were found in  $\approx 20$  nm thin LFO epitaxial films on (111) STO by DF TEM. The difference between the structural domains is that the orthorhombic  $a$  or  $b$  lattice parameters can be oriented parallel to either one of the substrate's  $[\bar{1}10]$ ,  $[\bar{1}01]$  or  $[0\bar{1}1]$  directions. However, since we are not able to discriminate between the orthorhombic  $a$  and  $b$  lattice parameters, it is still not clear if the film consists of more than 3 structural domains. However, dark contrast lines inside one-coloured regions, i.e. regions with similar diffraction patterns, indicate that further work is needed to fully understand the complete structure of the LFO film.

#### References

- [1] Wolf S A, Awschalom D D, Buhrman R A, Daughton J M, von Molnár S, Roukes M L, Chtchelkanova A Y and Treger D M 2001 *Science* **294** 1488–95
- [2] Nogués J and Schuller I K 1999 *J. Magn. Magn. Mater.* **192** 203–32
- [3] Kortright J, Awschalom D, Stöhr J, Bader S, Idzerda Y, Parkin S, Schuller I and Siegmann H C 1999 *J. Magn. Magn. Mater.* **207** 7–44
- [4] Baran E J 1990 *Catalysis Today* **8** 133–51
- [5] Haeni J H *et al.* 2004 *Nature* **430** 758–61
- [6] White R L 1969 *J. Appl. Phys.* **40** 1061–9
- [7] Geller S and Wood E A 1956 *Acta Cryst.* **9** 563–8
- [8] Glazer A M 1975 *Acta Crystallogr. A* **31** 756–62
- [9] Eibschütz M, Shtrikman S and Treves D 1967 *Phys. Rev.* **156**(2) 562–77
- [10] Lyubutin I S, Dmitrieva T V and Stepin A S 1999 *J. Exp. Theor. Phys.* **88** 590–7
- [11] Seo J W, Fullerton E E, Nolting F, Scholl A, Fompeyrine J and Locquet J P 2008 *J. Phys. Condens. Matter* **20**
- [12] Hallsteinsen I, Boschker J, Nord M, Lee S, Rzchowski M, Vullum P, Grepstad J, Holmestad R, Eom C and Tybell T 2013 *J. Appl. Phys.* **113**